

See discussions, stats, and author profiles for this publication at: <https://www.researchgate.net/publication/336880481>

Optimal Control Synthesis of Semi Active Vehicle Suspension

Article in IOP Conference Series Materials Science and Engineering · October 2019

DOI: 10.1088/1757-899X/618/1/012062

CITATIONS

0

READS

68

1 author:



Ivo Angelov

Technical University of Sofia

12 PUBLICATIONS 6 CITATIONS

SEE PROFILE

PAPER • OPEN ACCESS

Optimal Control Synthesis of Semi Active Vehicle Suspension

To cite this article: I Angelov 2019 *IOP Conf. Ser.: Mater. Sci. Eng.* **618** 012062

View the [article online](#) for updates and enhancements.

Optimal Control Synthesis of Semi Active Vehicle Suspension

I Angelov

Technical University of Sofia, 8 Kl. Ohridski Blvd, Sofia 1000, Bulgaria

E-mail: ivvoangelov@gmail.com

Abstract. The paper discusses the problems related with the synthesis of a linear quadratic (LQ) regulator of a semi active vehicle suspension. The synthesis combines the control through output variables with such by the input excitation i.e. classical LQ regulator with Compensator. The physical nonlinearities of the controllable magneto-rheological semi-active damper are taken into an account with the including in the feedback control circuit an inverse damper model. . A reduced suspension model is used to illustrate the synthesis (quarter car model).

1. Introduction

The quality criteria of the vibroisolation usually lay contradictory requirements for the vehicle's suspension synthesis. The ensuring enough ride comfort as generally requires a softer suspension, while the better vehicle stability and respectively better road-tire friction require a harder suspension. The compromise solutions in the conventional passive implementations are with limited possibilities. The usage of active or semi-active elements in vehicle suspensions gives considerable bigger potential in the solution of this problem. The semi-active vibroisolation is widely used because of its reliability, low price, and long exploitation period. It is known that due to the phase shifting, during some intervals of the oscillation time period, the damper directs energy into the object of vibroisolation instead of dissipating it. The main idea of the semi-active control is the reduction of the damping coefficient in these time period, which will decrease the amount of the energy transferred to the object [1÷4].

There are many types of the control laws [5÷8], but the main problem consists in the fact that, when the control is targeted to the comfort criterion the stability makes worse and vice versa. For this reason the synthesis of the optimal control requires a compromise solution satisfying both the quality factors simultaneously [9, 10, 11]. Generally the control based on a linear quadratic regulator - LQR is consider as an optimal and minimizes an integral of a time function formed by scaled variables describe the quality criteria [12÷16].

2. Dynamic model of the object

2.1. Quarter car model

On figure 1 is shown the quarter car suspension model (related to one of the wheels) with semi-active suspension, achieved by damper with controlled rheology. This model is enough adequate in case of constructive selection of the suspension performance, securing approximate independence of the motion of the front and the rear axis of the vehicle. At the same time due to its simplicity it is very appropriate for a real-time control. The results can be easily adapted for more complex models.



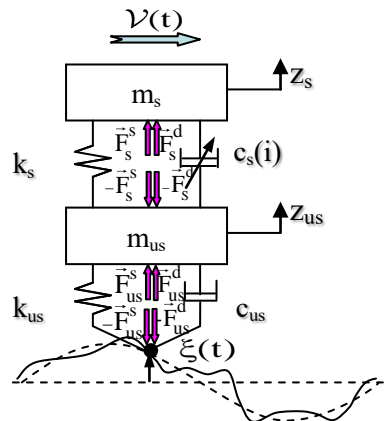


Figure 1. Quarter car model

Parameters of the model are:

z_{us} and z_s - vibro-displacements in the vertical plane of the sprung and unsprung masses.

m_{us} , m_s - sprung and unsprung masses;

k_{us} , k_s , c_{us} , $c_s(i)$ - tire and suspension spring and damping coefficients;

$$s(t) = \begin{cases} 0.5a_0t^2 & , 3a t < v_{max}^2 / a_0 \\ v_{max}^2 t - \frac{v_{max}^2}{2a_0} & , 3a t \geq v_{max}^2 / a_0 \end{cases} \quad \text{- motion law, } a_0 \text{ - acceleration, } v_{max}^2 \text{ - maximal velocity;}$$

$\xi(t) = \xi_h(s) + \xi_s(s)$ - kinematical excitation from the road roughness, presented as a sum of determined and stochastic component:

$\xi_h = H_h \sin(2\pi s / L)$ models the road roughness as a harmonic function with amplitude H_h (m) and wave length L (m),

$\xi_s(s)$ kinematical excitation modeling the road roughness according ISO 8608 [19];

\vec{F}_{us} , \vec{F}_s - forces transmitted through the tire to the unsprung mass and respectively from it to the sprung mass: $F_{us}^s = k_{us}(\xi - z_{us})$, $F_{us}^d = c_{us}(\dot{\xi} - \dot{z}_{us})$; $F_s^s = k_s(z_{us} - z_s)$, $F_s^d = f(i, z_{us}, z_s, \dot{z}_{us}, \dot{z}_s)$ where the indexes 's' and 'd' show respectively the spring and damping components and 'i' is the control signal.

2.2. Model of the semi-active damper

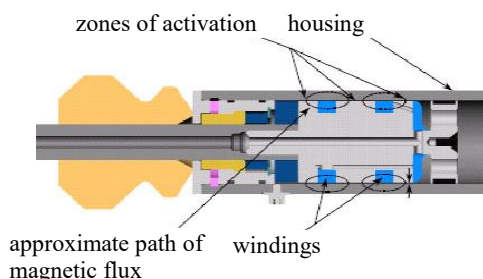


Figure 2. Scheme of MR damper

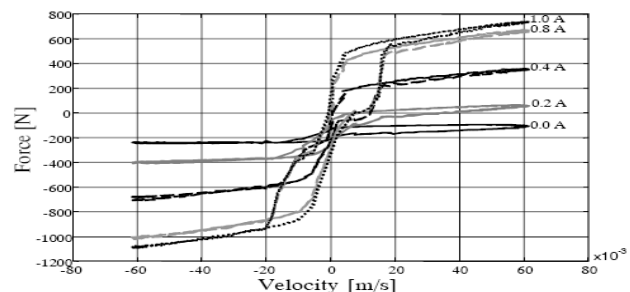


Figure 3. Performance of MR damper

The essence of the semi-active suspension consists in damper with variable rheology. The damping force depends on the kinematical performance on its deformation, and from the control signal.

The magneto-rheological (MR) dampers – figure 2 are more appropriate solution for the considered application. At them by feeding a control current signal is creates magnetic field which forms domains

from the ferrite micro particles, contained in silicon based suspension. In this way the damping coefficient becomes a function of the control signal and varying in definite boundaries.

The experimental performance, that show the dependency of the force vs. deformation velocity for different values of the control current, for MR damper type RD-1005-3 manufactured by „LORD Corporation”-USA are shown on the figure 3.

[20] proposes a dynamic model of controllable MR damper based on the approximation of the hysteresis suggested by Bouc-Wen [21, 22]. Its mechanical analogue is shown on figure 4.

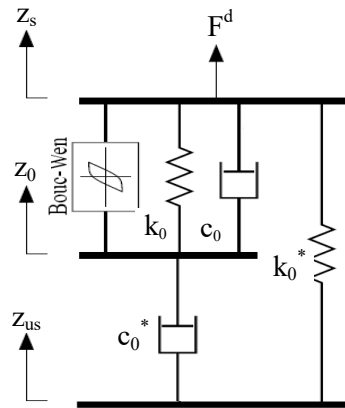


Figure 4. Bouc-Wen-Spenser mechanical model of MR damper

The damper force is calculated by the following equation:

$$F^d = k_0(z_0 - z_s) + c_0(\dot{z}_0 - \dot{z}_s) - k_h \zeta + k_0^*(z_{us} - z_s + \delta_0) = k_0^*(z_{us} - z_s + \delta_0) - c_0^*(\dot{z}_0 - \dot{z}_{us}), \quad (1)$$

where k_h (N/m) is the elastic coefficient connected with the value on which the angle of the characteristic is changed and δ_0 (m) takes into account the hydraulic accumulator.

From the force balance upon the level z_0 is obtained:

$$\dot{z}_0 = [c_0^* \dot{z}_{us} + c_0 \dot{z}_s - k_0(z_0 - z_s) + k_h \zeta] / (c_0 + c_0^*). \quad (2)$$

The evolutionary variable is given by the dependency:

$$\dot{\zeta} = -\gamma |\dot{z}_0 - \dot{z}_s| |\zeta|^\chi + \beta (\dot{z}_0 - \dot{z}_s) |\zeta|^\chi - \nu (\dot{z}_0 - \dot{z}_s) = \left\{ [\beta - \text{sign}((\dot{z}_0 - \dot{z}_s) \zeta) \gamma] |\zeta|^\chi - \nu \right\} (\dot{z}_0 - \dot{z}_s), \quad (3)$$

where γ (m), β (m), ν and χ are coefficients forming the hysteresis.

The values of k_h , c_0 and c_0^* as functions of the control current are given by the first order approximations:

$$k_h = k_h^c + k_h^v i', \quad c_0 = c_0^c + c_0^v i', \quad c_0^* = c_0^{*c} + c_0^{*v} i'. \quad (4)$$

Here i' is function taking into account the process of rheological equilibrium after the aperiodic dependency from first order:

$$i' = (i - i') / \tau_r, \quad \tau_r - \text{time-sample of the process}, \quad i \in [0, i_{max}]. \quad (5)$$

2.3. Inverse model of MR damper

The MR damper has essential nonlinear characteristics and physical limitations. For the control purpose an inverse dynamical model is required. For a particular state of the system the model assures corresponding optimal damper force, calculated by the controller. It is obvious that due to the physical

limitations, the optimum force will not be generated in some situations and generally the control will be quasi-optimal.

Due to the complexity of the problem, a neural network model is used [12, 23, 24]. Its structure is shown on figure 5.

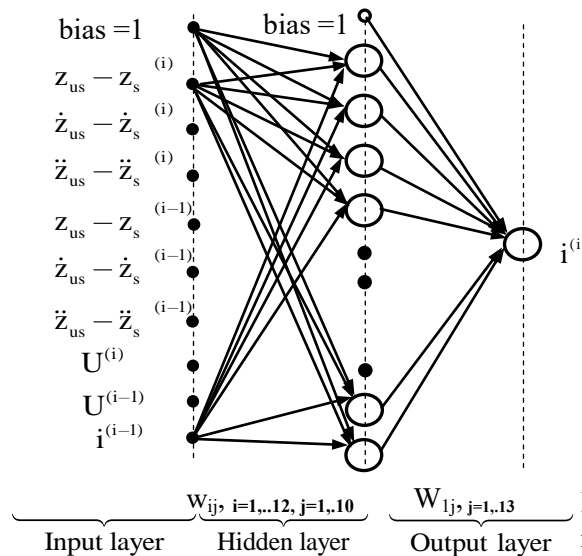


Figure 5. Inverse neural networks model of MR damper

In the input layer the value of the deformation of the damper and its first and second derivatives with respect to time are entered, as well as the control signal U (the damper force). The output layer represents a linear activation function and determines the control current, which generates the current damper force U_i .

The hidden layer consists of 12 neurons with non-linear logical sigmoid activation functions $g_i(x) = \frac{\theta}{1 + e^{-\sigma x}} - 1$, where $\theta = 2$, and σ is positive constant. The determination of the weight coefficients for the hidden layer W_{ij} , $i=1,..,12$, $j=1,..,10$ and the output layer W_{lj} , $j=1,..,13$, is done by the Levenberg-Margquardt method and the Jacobian is calculated by back propagation method [25].

2.4. State space presentation

$$\begin{aligned} \dot{X} &= AX + B_A \Lambda + B_U U, \quad X(0) = X_0 \\ Y &= CX + D_A \Lambda + D_U U \end{aligned} \tag{6}$$

where:

- ♦ $X = [z_{us} \quad z_s \quad \dot{z}_{us} \quad \dot{z}_s]^T$ - state vector; $\Lambda = [\xi, \dot{\xi}]^T$ - input excitation; $U = F_s^d$ - the control;
- ♦ $Y = [z_{us} \quad z_s \quad -F_{us} \quad \ddot{z}_s]^T$ - output vector which consists of characteristics that define the quality of the suspension – the motions z_{us} and z_s , the dynamical component of the normal force $-F_{us}$, which determines the friction tire-road and the acceleration of the sprung mass \ddot{z}_s which determines the ride comfort;
- ♦ matrices of the state A , the control B_U and the input B_A are :

$$A = \begin{bmatrix} 0_{2 \times 2} & I_2 \\ -m^{-1}k & -m^{-1}c \end{bmatrix}, \quad B_U = \begin{bmatrix} 0_{2 \times 1} \\ m^{-1}d_U \end{bmatrix}, \quad B_A = \begin{bmatrix} 0_{2 \times 2} \\ m^{-1}d_A \end{bmatrix};$$

- ♦ and the matrices of the output variables are:

Combining (10)÷(12) are obtained two Riccati equations (for $K=\text{const}$ and $\Psi=\text{const}$):

$$\begin{cases} \tilde{K}A + A^T\tilde{K} + Q_U - (\tilde{K}B_U + N_{XU})R_U^{-1}(N_{XU}^T + B_U^T\tilde{K}) = 0 \\ \tilde{\Psi} = -\left[A^T - (\tilde{K}B_U + N_{XU})R_U^{-1}B_U^T\right]^{-1}\left[(\tilde{K}B_U + N_{XU})R_U^{-1}N_{U\Lambda} - (\tilde{K}B_\Lambda + N_{X\Lambda})\right]\Lambda = 0 \end{cases} \quad (13)$$

Matrix \tilde{K} is defined by (13) based on the numerical computation of the vectors of Hamiltonian matrix [26].

Combining (11), (12) and second equation of (13) is obtained the optimal control:

$$\begin{cases} U_{\text{opt}} = -G_X X - G_\Lambda \Lambda \\ G_X = R_U^{-1}(N_{XU}^T + B_U^T K) \\ G_\Lambda = R_U^{-1}\left\{N_{U\Lambda} + B_U^T\left[A^T - G_X^T B_U^T\right]^{-1}\left[G_X^T N_{U\Lambda} - (\tilde{K}B_\Lambda + N_{X\Lambda})\right]\right\} \end{cases} \quad (14)$$

The kinematic excitation due to the road roughness may be identified using the accelerations of the sprung and unsprung masses obtained from accelerometers:

$$\tilde{\xi} = w_{us}(s)\tilde{z}_{us} + w_s(s)\tilde{z}_s, \quad (15)$$

where transfer functions are: $w_{us}(s) = \frac{m_s s^2 + c_{us}s + k_{us}}{s^2(c_{us}s + k_{us})}$, $w_s(s) = \frac{m_s}{c_{us}s + k_{us}}$ and with \sim is denoted the Laplace transform image.

On figure 6 is given the structural scheme of the control.

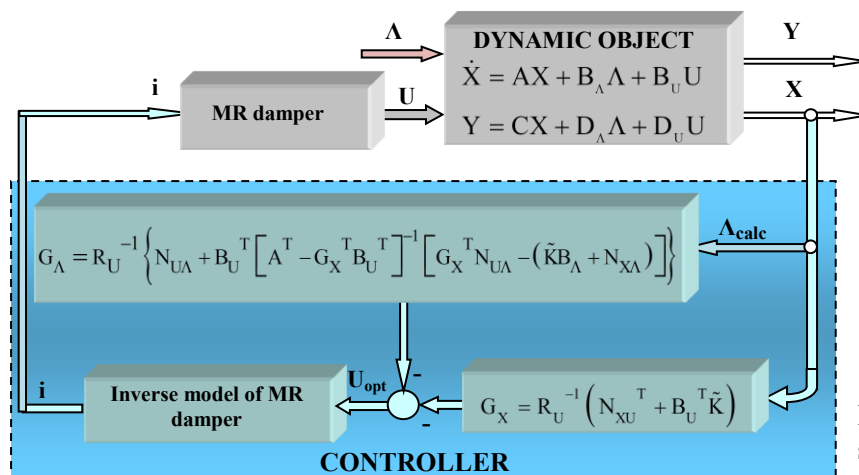


Figure 6. Structural scheme of the control

4. Numerical example

4.1. Description of the task

- It is consider a model with the following characteristics:

$$m_1=40 \text{ kg}; m_2=350 \text{ kg}; k_1=1.6e^5 \text{ N/m}; k_2=0.19e^5 \text{ N/m}; c_1=110 \text{ Ns/m}.$$

- The parameters of the MR damper model are given in table 1

Table 1. Parameters of the MR damper model

c_0^c , Ns/m	c_0^v , Ns/mA	k_0 , N/m	k_h^c , N/m	k_h^v , N/mA	c_0^{*c} , Ns/m	c_0^{*v} , Ns/mA	k_0^* , N/m
780	2230	1400	14500	71500	28000	500	540
χ	τ_r , s	γ , m ⁻²	β , m ⁻²	δ	δ_0 , m	i_{max} , A	
2	0,0053	0,5 10 ⁶	0,8 10 ⁶	170	0	1,2	

- ♦ The parameters of the motion law are: $a_0=1.1$ m/s², $v_{max}=130$ km/h, $T_k=25$ s.
- ♦ The kinematic excitation due to the road roughness as function of the time is shown on figure 7.

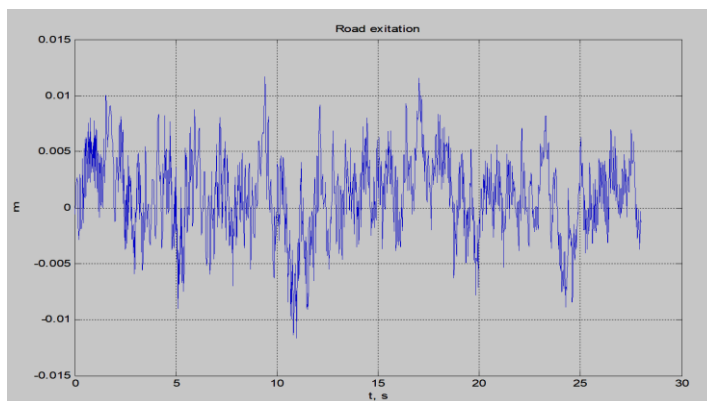


Figure 7. Kinematic excitation vs. time

- ♦ The weighted matrix in the object function are

$$Q=\text{diag}([1.34e4, 0.258e4, 2.462e-6, 3.453]), R=1.38e-6.$$

4.2. Results

Characteristics	Passive suspension $b_2=1505$ Ns/m		With semi active LQR control	
	Z_{us}	Z_{us}	Z_{us}	Z_{us}
$\int_0^{T_k} Z(t)dt$, ms	0,346	0,23	0,378	0,0658
Max(Z , Ż , Z̈), [m,m/s,m/s ²]	[0,027;1,03;79,3]	[0,036;0,27;4,67]	[0,031;1,32;104,5]	[0,005;0,12;7,84]
RMS(Z, Ż, Z̈) [m,m/s,m/s ²]	[0,011;0,29;16,4]	[0,01;0,082;1,5]	[0,012;0,34;24,1]	[0,022;0,04;1,66]
RMS(F_{us}^d), N		797		768,9
J		0,01602		0,01322

Acknowledgements: This work was supported by OP "Science and education for smart growth" – centers of excellence TU Sofia „National center of Mechatronics and clean technologies”, BG05M2OP001-1.001-0008-C01 Sect. Design, synthesis and testing of noise and vibration protection

References

[1] Karnopp D, 1983 Active Damping in Road Vehicle Suspension Systems *Vehicle System Dynamics* **12** pp 291-316

[2] Karnopp D, 1990 Design principles for vibration control systems using semi-active dampers *Transactions of the ASME - J. Dynamic Systems, Measurement, and Control* **112** pp 448-455

[3] Yi K., Wargelin M., Hedrick K. 1992 Semi-active suspensions to reduce road damage: theoretical design and implementation, in *Heavy vehicles and roads: technology, safety and policy* Thomas Telford London pp 122-129

[4] Genov J. et al. 2008 Analysis and Control Laws of Semi-Active Vehicle Suspension System

- with Rending an account of the Physical Characteristics of Magneto-Rheological Dampers *Proc. of the 13th Int. Conf. on Applied Mechanics and Mechanical Engineering (AMME-13) 27-29 May 2008 M.T.C. Cairo Egypt* pp 1333-1348
- [5] Ahmadian M. 1997 Hybrid Semiactive Control to Secondary Suspension Applications *Proc. of Six ASME symposium on Advanced Automotive Technologies Texas 1997* pp 1-8
- [6] Guglielmino E. et al. 2008 *Semi-active Suspension Control - Improved Vehicle Ride and Road Friendliness* Springer-Verlag London Ltd. p 302
- [7] Savaresi S. et al. 2010 *Semi-Active Suspension Control Design for Vehicles* Butterworth-Heinemann is an imprint of Elsevier Ltd. Oxford UK p 232
- [8] Preumont A. 2011 *Vibration Control of Active Structures an Introduction* Springer p 453
- [9] Venkov G., Tashkov S., Genov J. 2007 Optimal Multicriterial Synthesis of Vehicle Suspension *Proc. of the 32-st Int. Conf. Applications of Mathematics in Engineering and Economics '32, Sozopol, Bulgaria, 2006* Softrade, Sofia pp 217-221.
- [10] Genov J., Tashkov S. 2015 Multi-Objective Synthesis of Vehicle Semi-Active Suspension Control Represented In A Vertical Plane Part 1 Model and Algorithm for Multi-Objective Synthesis *Proc. of Sc. Conf. on Aeronautics, Automotive and Railway Eng. and Technologies BulTrans-2015*, TU-Sofia pp 77-83
- [11] Mastinu G., Gobbi M., Miano C. 2006 *Optimal Design of Complex Mechanical Systems. With Applications to Vehicle Engineering*, Springer-Verlag Berlin Heidelberg p 392
- [12] Genov J., Tashkov S., Venkov G., 2009 On the Synthesis of Optimal and Quazi-optimal Control of Semi-Active insulation System *35th Int. Conf. Appl. of Math. in Eng. and Economics - AMEE-2009*, AIP Conference Proceedings **1184** pp 32-38.
- [13] Genov J. et al. 2009. On the Synthesis of Optimal and Quazi-Optimal Control of Semi-Active Vibro-insulation System *11th National Congress on Theoretical and Applied Mechanics, 2-5 Sept. 2009, Borovets Bulgaria* pp 1-12
- [14] Nguyen T.-A. 2006 *Application of Optimization Methods to Controller Design for Active Suspensions* Doktor-Ingenieurs genehmigte Dissertation TU Cottbus p 152;
- [15] Genov J., Tashkov S. 2012 Quasi Optimal Control of Magneto-rheological Damper. *Proc. of Int. Conf. and Exh. on New Actuators and Drive Systems ACTUATOR 12, Bremen, Germany, 18-20 June 2012* pp 612-615
- [16] Pareto V. 1896 *Cours D'économie politique Tome Premier* F. Rouge Libr. Édit. Lausanne p 438
- [17] Pareto V. 1897 *Cours D'économie politique Tome Second* F. Rouge Libr. Édit. Lausanne p 430
- [18] Genov J., Tashkov S. 2015 Multi-Objective Synthesis of Vehicle Semi-Active Suspension Control Represented in a Vertical Plane Part 2 Synthesis of Linear Quadratic Regulator *Proc. of Sc. Conf. on Aeronautics, Automotive and Railway Eng. and Technologies BulTrans-2015* pp 84-88
- [19] International Standard ISO 8608 1995 *Mechanical vibration and shock – Road Surface Profiles Reporting of Measured Data*, Int. Org. of Standardization Central Secr., Switzerland, p 30
- [20] Spenser Jr., B. et al. 1997 Phenomenological Model of a Magnetorheological Damper *Journal of Engineering Mechanics* **123** pp 230-238
- [21] Bouc R. 1967 Forced vibration of mechanical systems with hysteresis. *Proceedings of the Fourth Conference on Non-linear oscillation, Prague, Czechoslovakia* p 315
- [22] Wen Y. 1976 Method for random vibration of hysteretic systems *J. Eng. Mech.* **102** pp 249-263
- [23] Kim B., Roschke P. 1999 Linearization of Magnetorheological Behaviour Using a Neural Network *Proc. of the American Control Conf., San Diego, June 1999* AACC pp 4501-4505
- [24] Gilev B., Venkov G., Genov J. 2006 Neural Network Prediction of Hysteresis, *Proc. of the 31-st Int. Conf. Appl. of Math. in Eng. and Economics '31, Sozopol' 2005*, Softrade pp 172-175
- [25] Hinton G. 2013 *Computation in Neural Networks [Lecture course CSC2535](#)*, Dept. of Computer Science, University of Toronto, Canada
- [26] Arnold W., Laub A. 1984 Generalized Eigen problem Algorithms and Software for Algebraic Riccati Equations, *Proc. IEEE*, **72**, No.12, pp 1746-1754